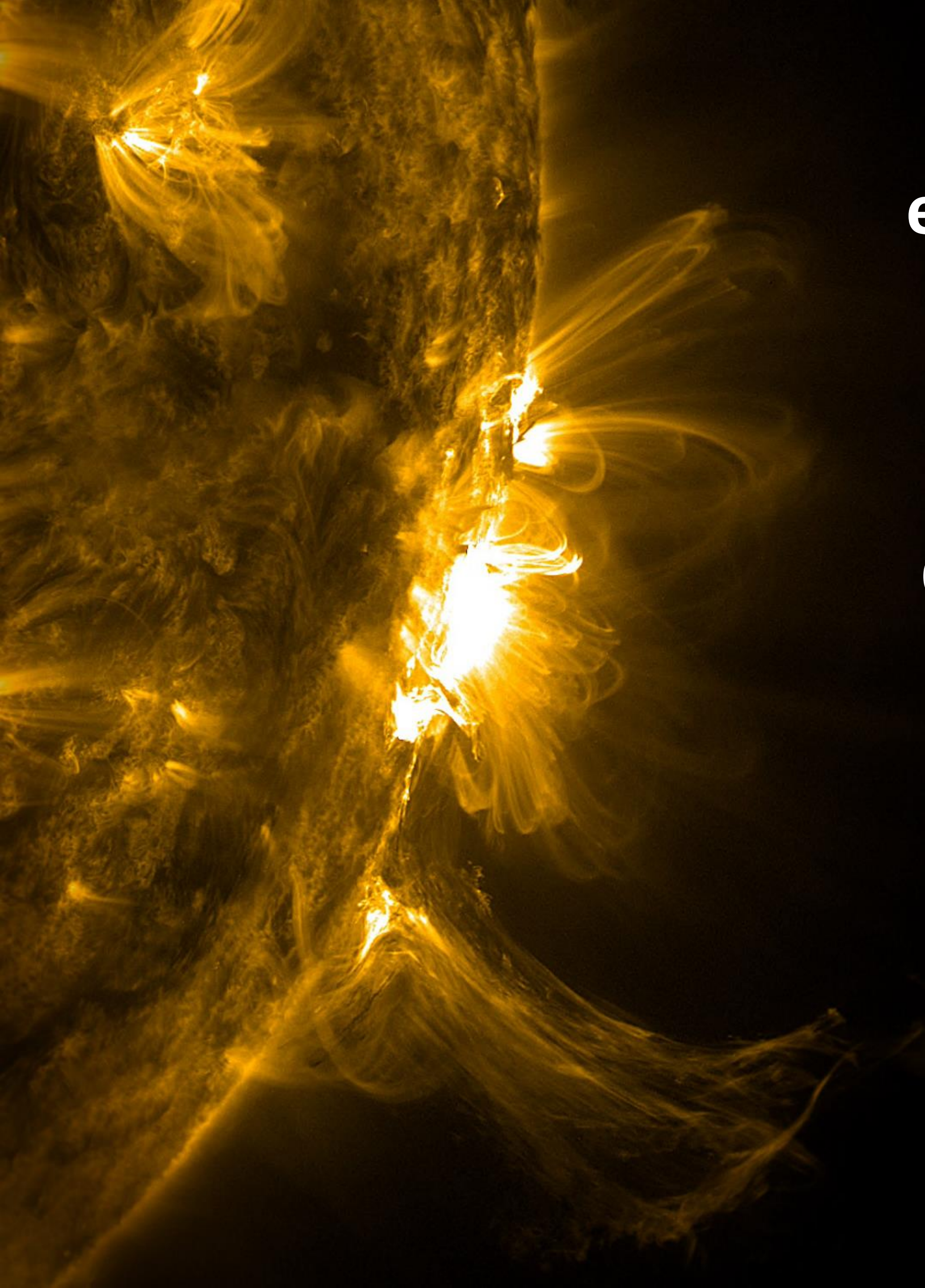

The Effects of Non-equilibrium Processes on Line Formation in the Lower Transition Region and Upper Chromosphere Relevant to IRIS

Stephen J. Bradshaw
Rice University
Paola Testa (part 1)
CfA / LMSAL
Shah Bahauddin (part 2)
UC Boulder / NSO

IRIS 10, 5th November 2019

i. Outline

1. Signatures of Coronal Heating
    a. IRIS Observations
    b. Numerical Investigation
    c. NEQI and Density-Dependence
2. Heating in the Transition Region
    a. IRIS Observations
    b. Numerical Investigation
3. Summary of Findings

1. Signatures of Coronal Heating

The "smoking gun" of impulsive coronal heating is predicted to be the detection of radiating hot plasma at temperatures near 10 MK

Imaging instruments (e.g. SDO/AIA) don't have sufficient temperature discrimination to unambiguously identify the hot emission, but spectroscopic instruments (e.g. EUNIS[1]) do

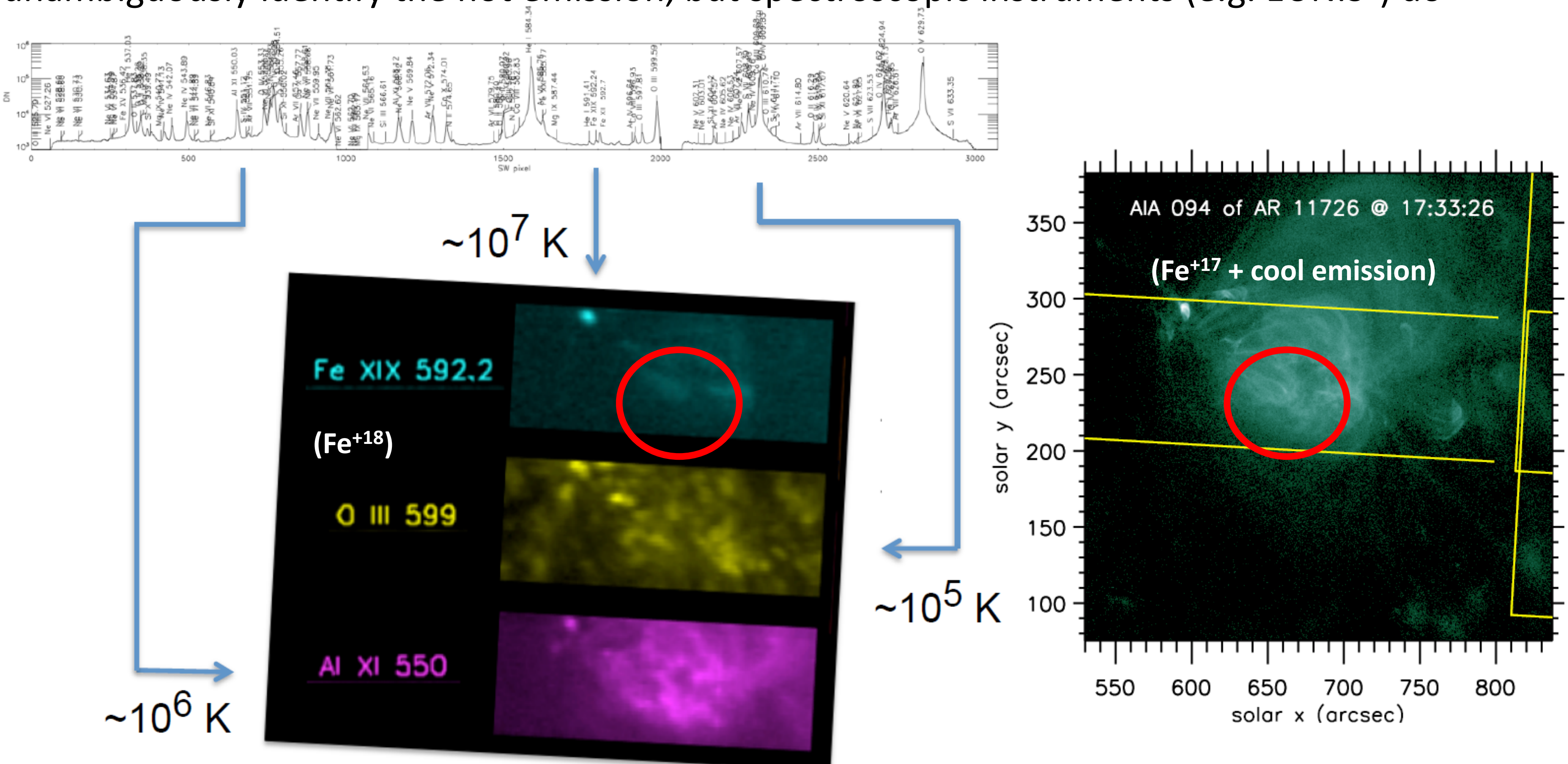

[1] Brosius, J. W., et al. 2014, ApJ, 790, 112

Hot coronal emission is difficult to detect because:

- The hot plasma has a low density
- It cools quickly, by thermal conduction, before significant coronal filling occurs
- It cools before a substantial population of strongly charged ions can be created

Numerical simulation of five minutes during coronal loop heating ($\tau_H = 10$ s) predicted in a hot (EUV) emission line detected by Hinode/EIS. The maximum temperature reached by the plasma is about 7 MK

Predicted intensity in equilibrium (non-equilibrium) ionization is shown in the upper (lower) plot. In non-equilibrium the emission appears ≈ 90 s after heating

We will soon explore the X-ray corona with spatially and spectrally resolved observations using the Marshall Grazing Incidence X-ray Spectrometer (MaGIXS)[2] in 2020

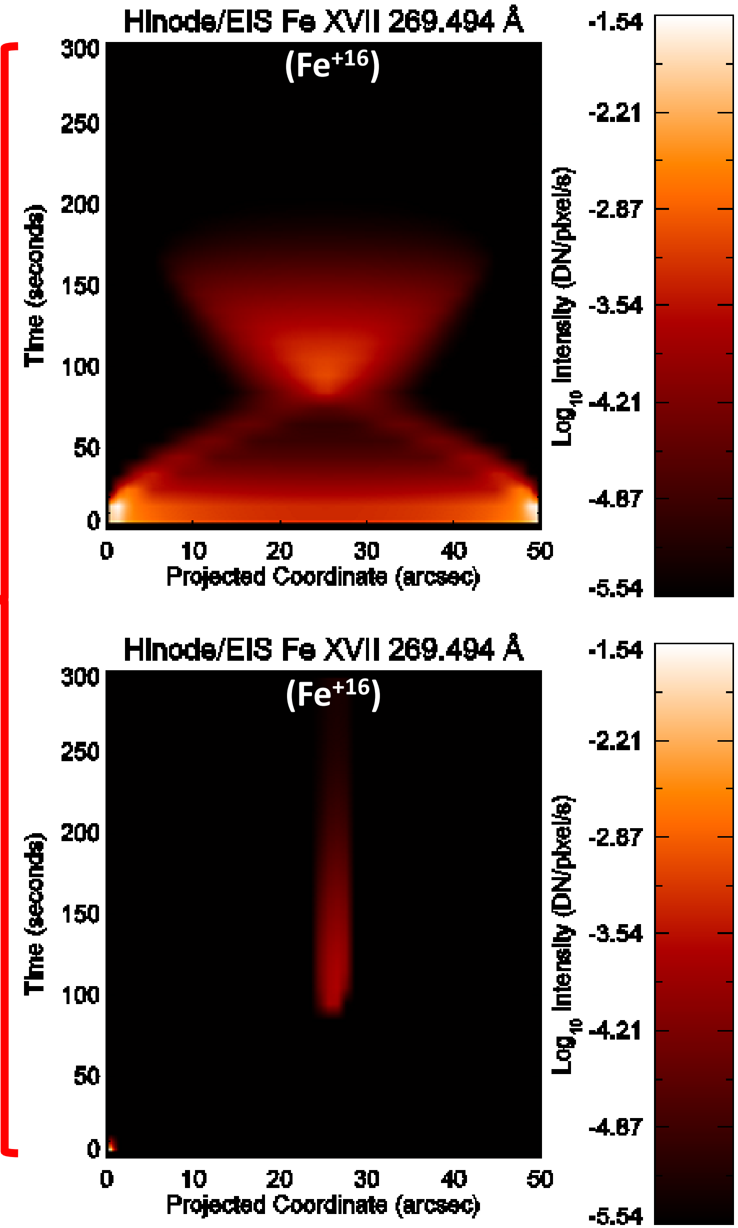

[2] Champey, P. R., et al. 2016, Proc. SPIE Conf. Ser., 9905, 73

Intermediate-frequency heating[3]

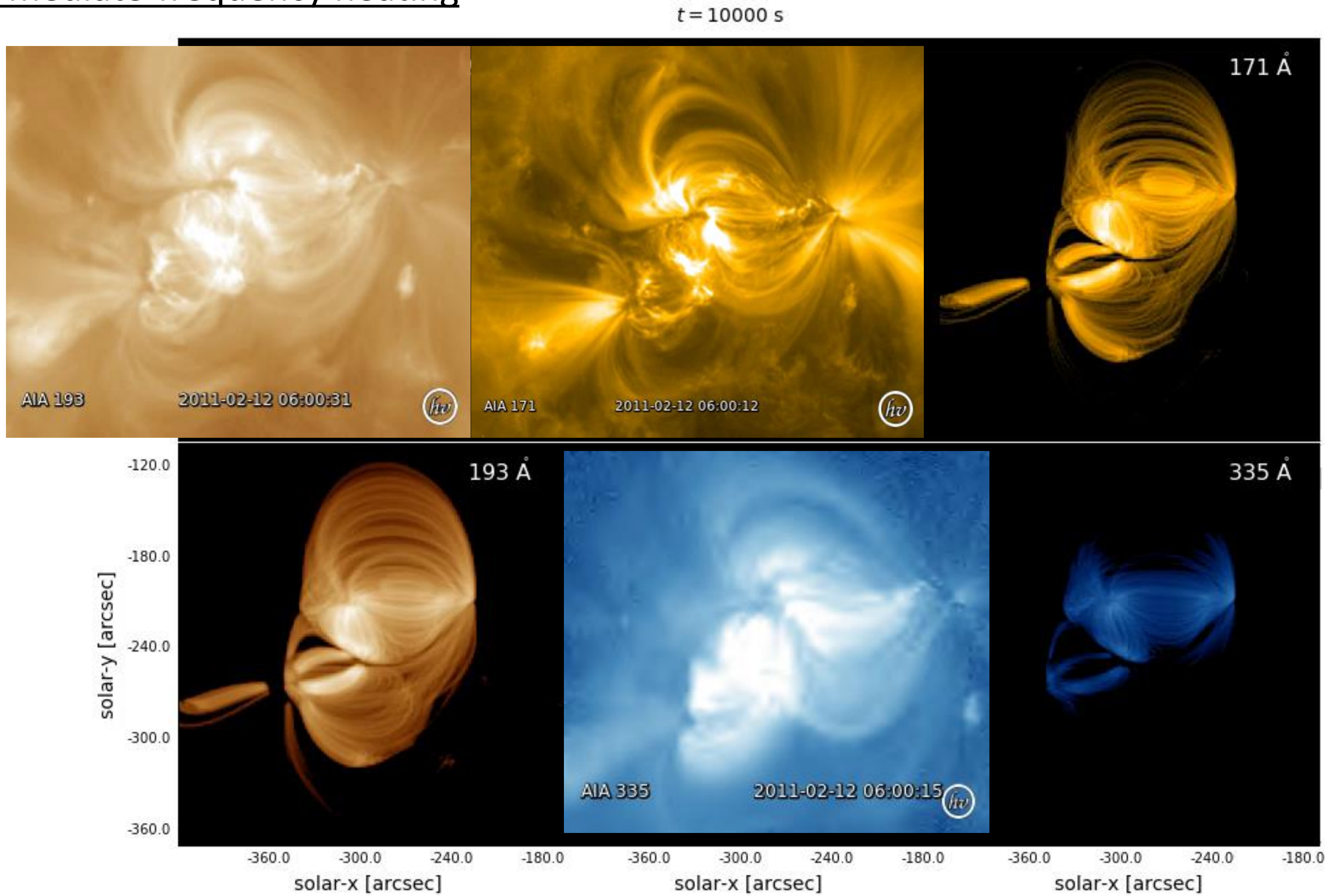

[3] Barnes, W. T., et al. 2019, ApJ, 880, 56

- Numerical models of impulsive heating predict temperatures in the range of 3-5 MK at the onset of radiative cooling.
- Higher temperature (> 7 MK) plasma would be strong evidence for impulsive heating
- Difficult to observe: low density; thermal conduction; non-equilibrium ionization
- Can we find signatures of impulsive heating to diagnose by looking elsewhere?

1a. IRIS Observations

- The transition region and corona are very strongly coupled to each other via sound waves[4]
- Disturb one, disturb the other… But, the transition region is more dense, the emission brighter, and the ions already present
- Nonetheless, we expect the emission spectrum to be strongly decoupled from the local temperature → non-equilibrium
- Coronal signatures are hard to detect; transition region signatures are hard to predict and interpret, but now we have a chance
- Focus on three processes that may each play a key role in forming the emission lines observed by the Interface Region Imaging Spectrograph (IRIS)[5]:
    - Non-equilibrium ionization
    - Density-dependence of collisional processes (e.g. quenching)
    - Streaming electrons creating high-energy tail populations

[4] Cargill, P. J., & Bradshaw, S. J. 2013, ApJ, 772, 40; [5] De Pontieu, B., et al. 2014, SoPh, 289, 2733

AR 12593

AR 12595

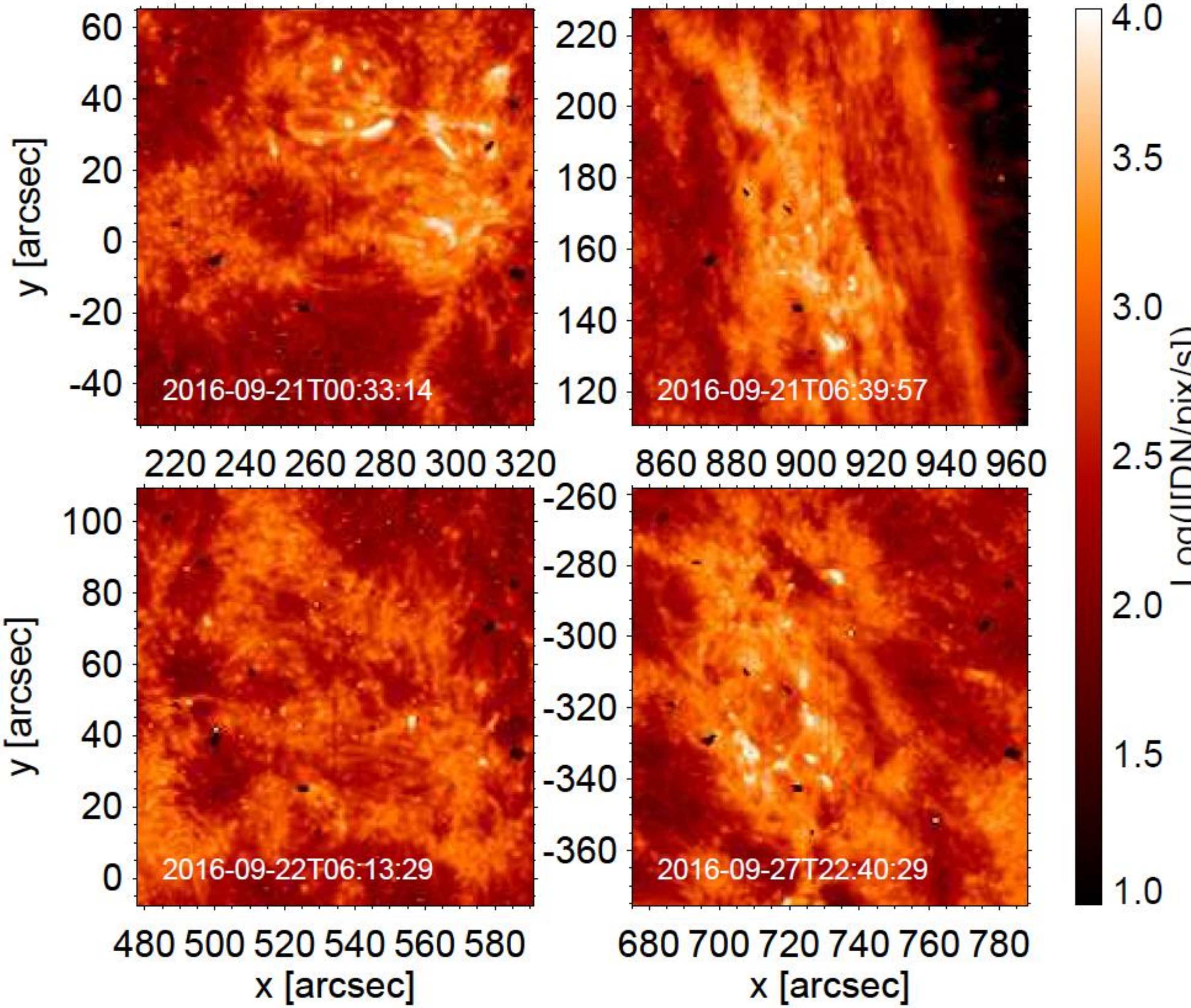

AR 12593

AR 12597

IRIS SJI 1400 Å (red)
$\log_{10} T(\mathrm{K}) = 4.7 - 5.2$

AIA 171 Å / Fe IX (green)
$\log_{10} T(\mathrm{K}) = 5.9$

AIA 335 Å / Fe XVI (blue)
$\log_{10} T(\mathrm{K}) = 6.5$

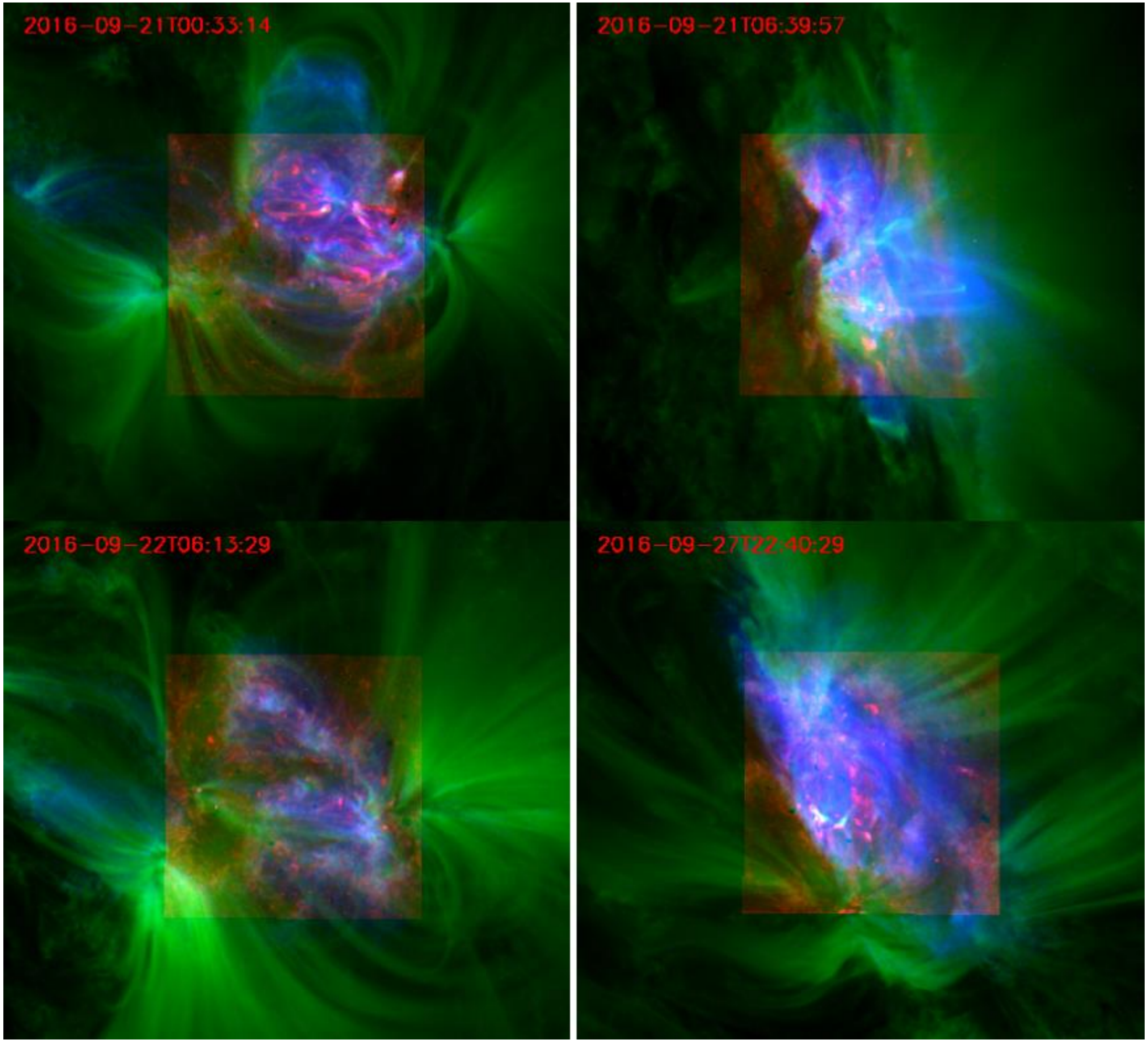

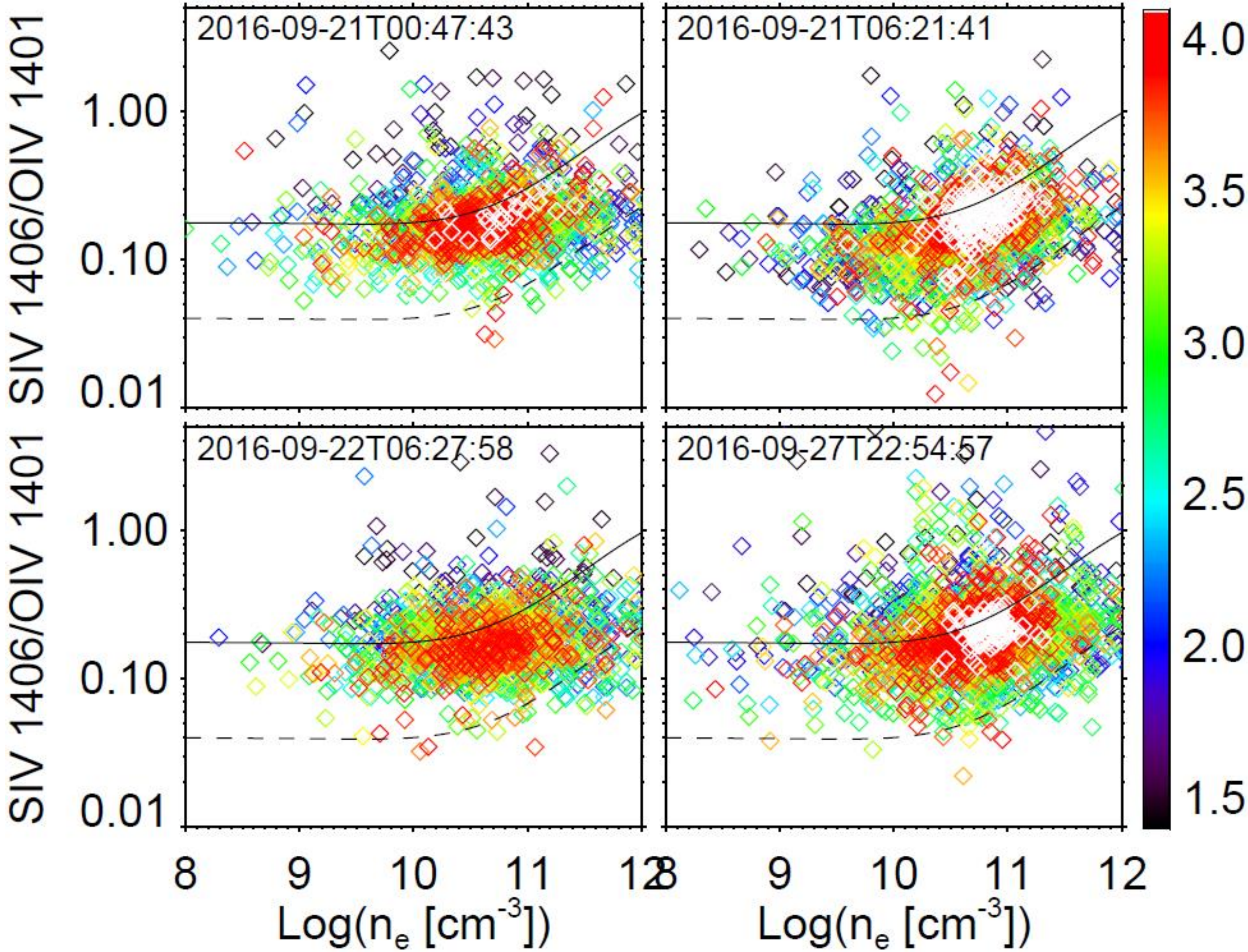

2016-09-21T00:47:43
2016-09-21T06:21:41
2016-09-22T06:27:58
2016-09-27T22:54:57
SIV 1406/OIV 1401
1.00
0.10
0.01
8
9
10
11
12
Log(n_e [cm^-3])
Log(I OIV 1401 [DN])
4.0
3.5
3.0
2.5
2.0
1.5

1b. Numerical Investigation

- Conduct a set of numerical experiments[6] to investigate the transition region response to coronal heating
- Take account of key (aforementioned) atomic processes that contribute to line formation
- Ascertain which make the dominant contribution
- Use model findings / results to:
    - Recognize clear signatures of coronal heating in transition region spectra
    - Guide interpretation of observations to extract information regarding properties of the underlying mechanism
    - Identify reliable spectroscopic diagnostics and understand their associated ranges of uncertainty and validity

[6] Bradshaw, S. J., & Testa, P. 2019, ApJ, 872, 123

Two trains composed of ten impulsive heating events. The first train weakly heats the plasma to temperatures ≈ 4 MK, the second train strongly heats the plasma to temperatures ≈ 10 MK.

Red – e^- temperature
Blue – H temperature
Black – e^- density

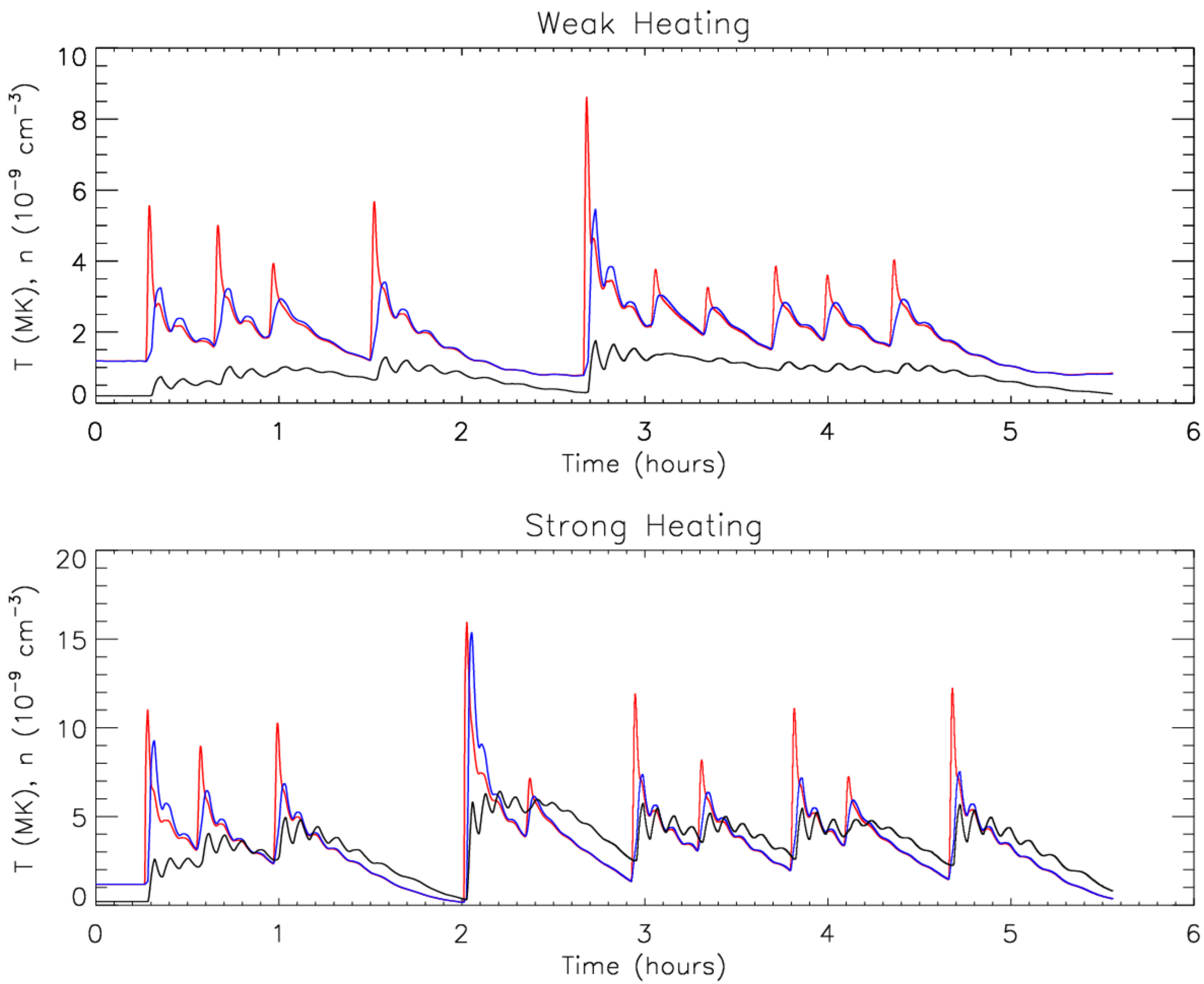

1c. NEQI and Density-Dependence

<u>ADAS[7] Rates, Weak Heating</u>

The intensity of the S IV (1406.060 Å) and O IV (1401.163 Å) lines in the IRIS passband calculated for ionization and recombination rates in the low-density limit, and when density-dependence is considered, for equilibrium and non-equilibrium ionization.

(Note: these are line-integrated intensities)

Red – low-density limit
Blue – density dependent

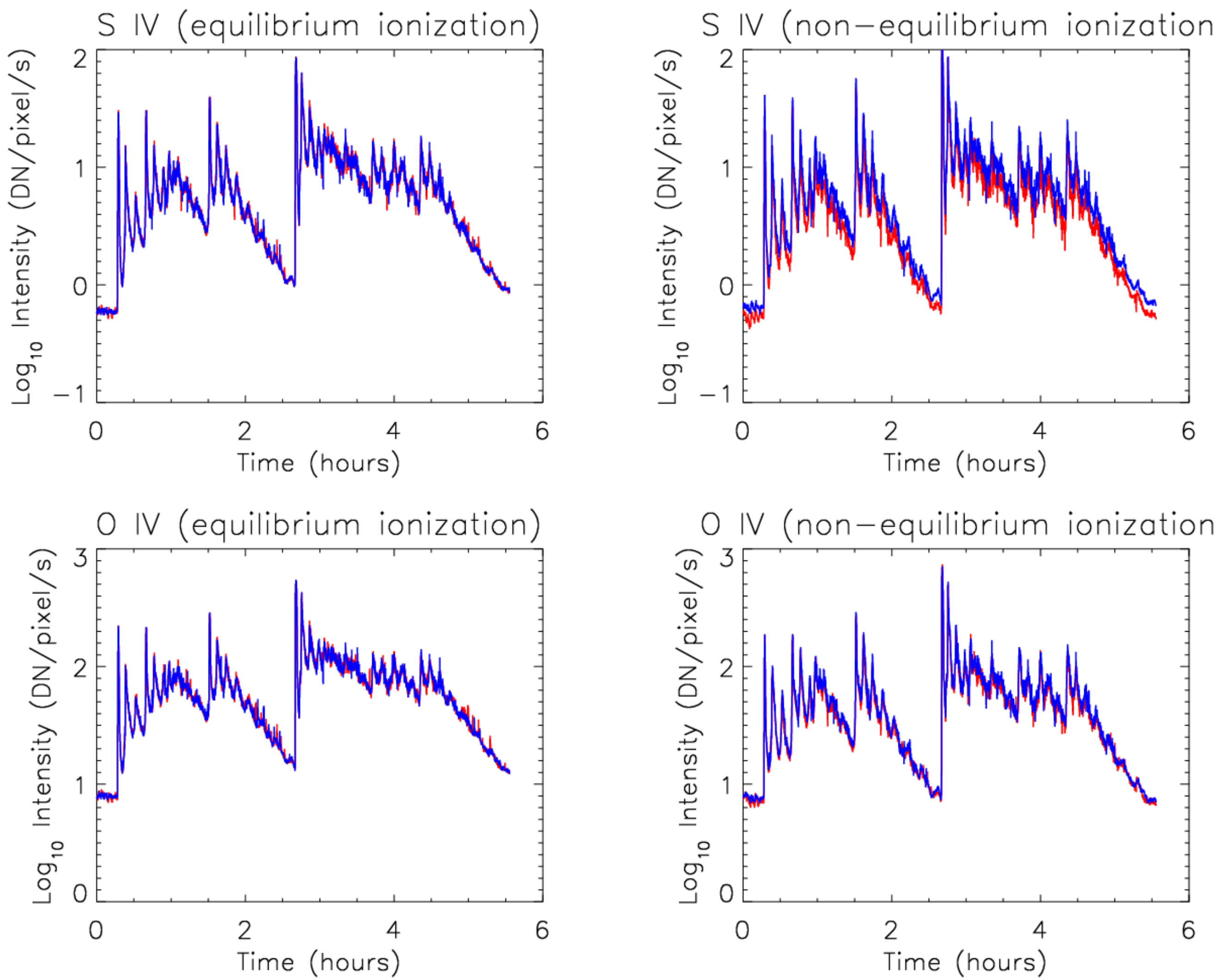

[7] Summers, H. P., et al. 2006, Plasma Physics and Controlled Fusion, 48, 263

<u>ADAS Rates, Weak Heating, Low Density Limit</u>

The electron density calculated from line-of-sight integrated, density sensitive, line ratios.

Red – equilibrium ionization
Blue – non-equil. ionization

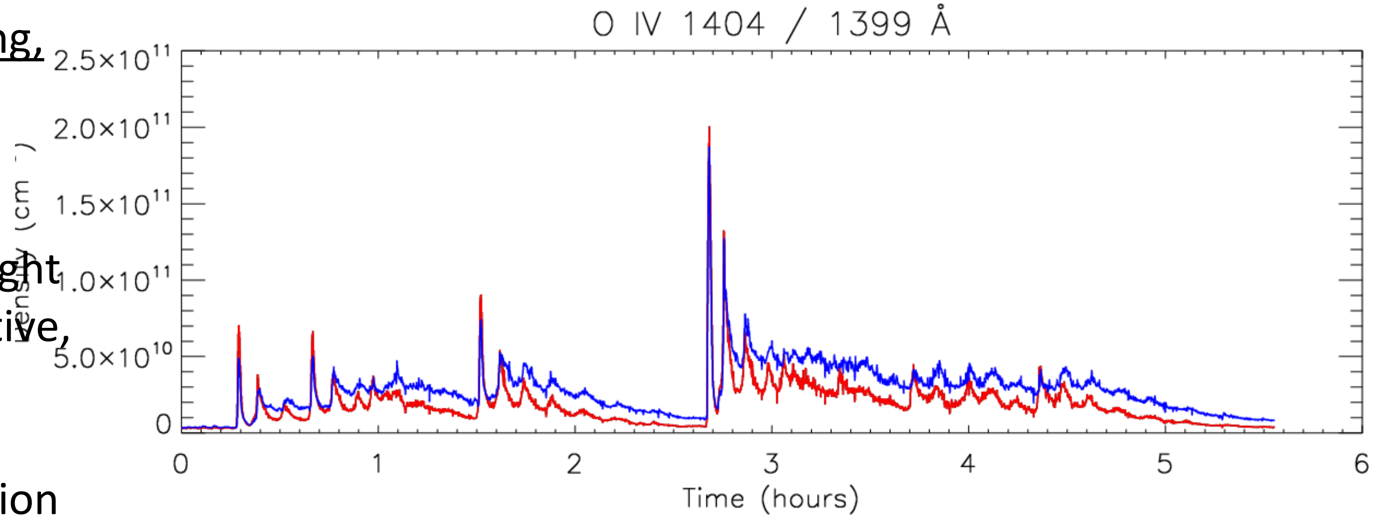

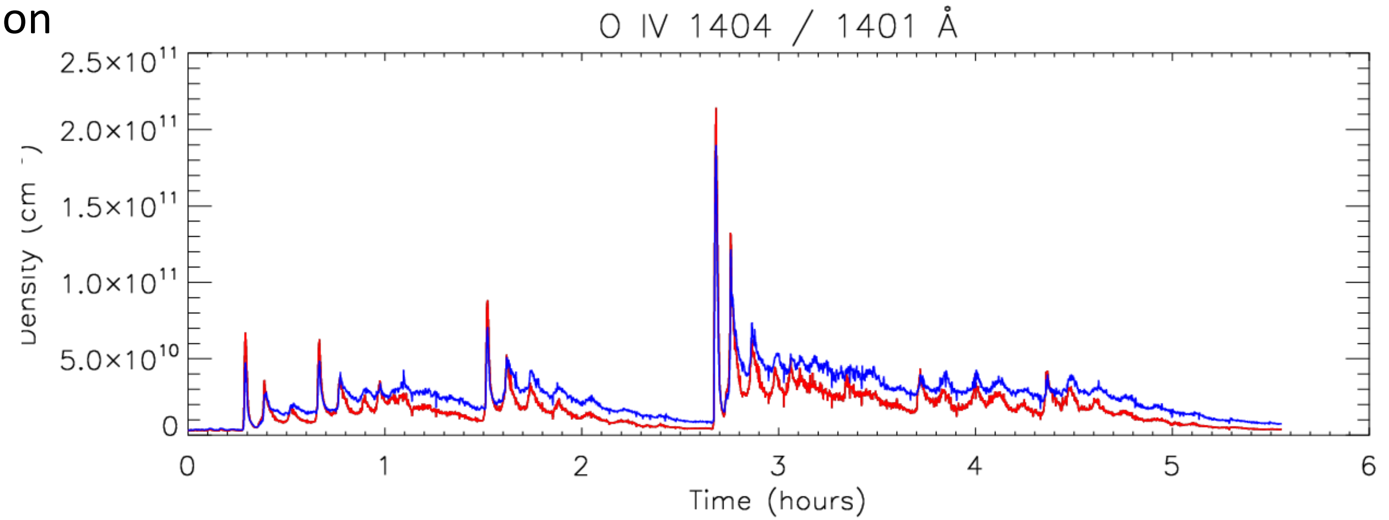

ADAS Rates, Weak Heating, Density-Dependent

The electron density calculated from line-of-sight integrated, density sensitive, line ratios.

Red – equilibrium ionization
Blue – non-equil. ionization

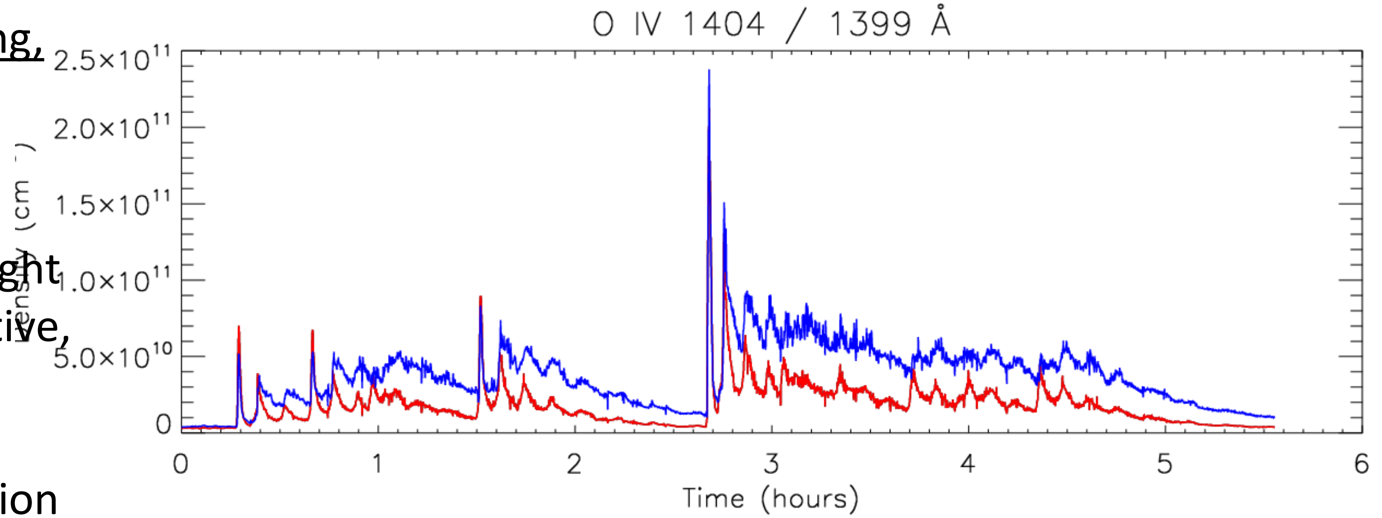

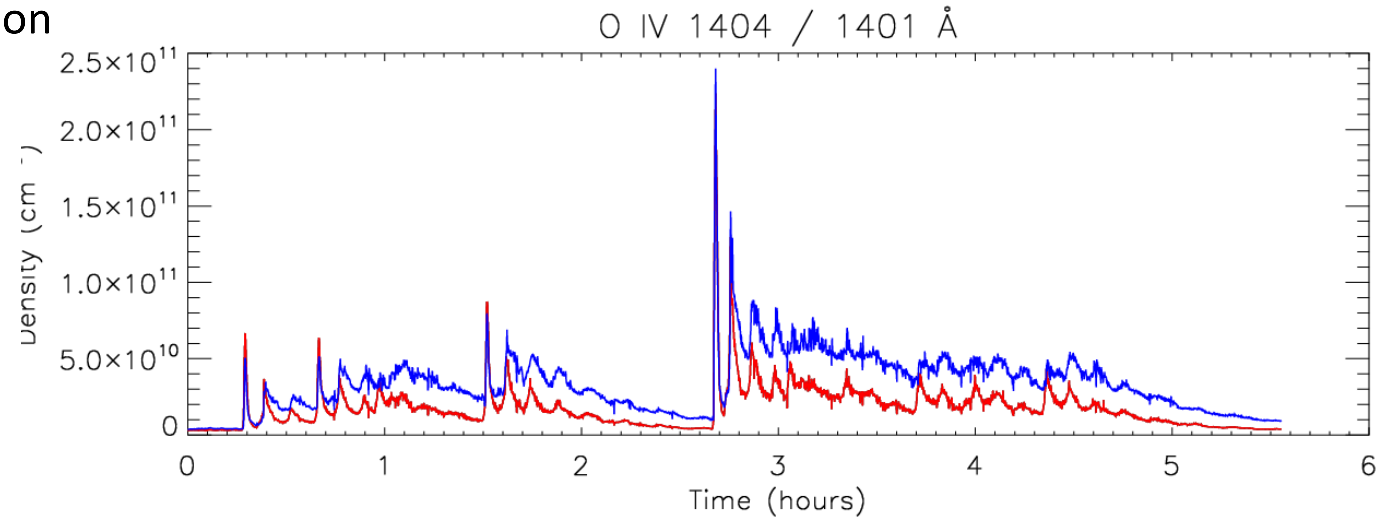

ADAS Rates, Weak Heating, Low Density Limit

The intensity ratios of the S IV (1406.060 Å) and O IV (1401.163 Å) lines plotted as a function of the electron density calculated using the O IV (1404.806 / 1399.776 Å) line ratio.

Solid: Chianti[8,9]-predicted ratio at the S IV equilibrium formation temperature ($\log_{10}T = 5.0$ K).

Dashed: Chianti-predicted ratio at the O IV equilibrium formation temperature ($\log_{10}T = 5.15$ K).

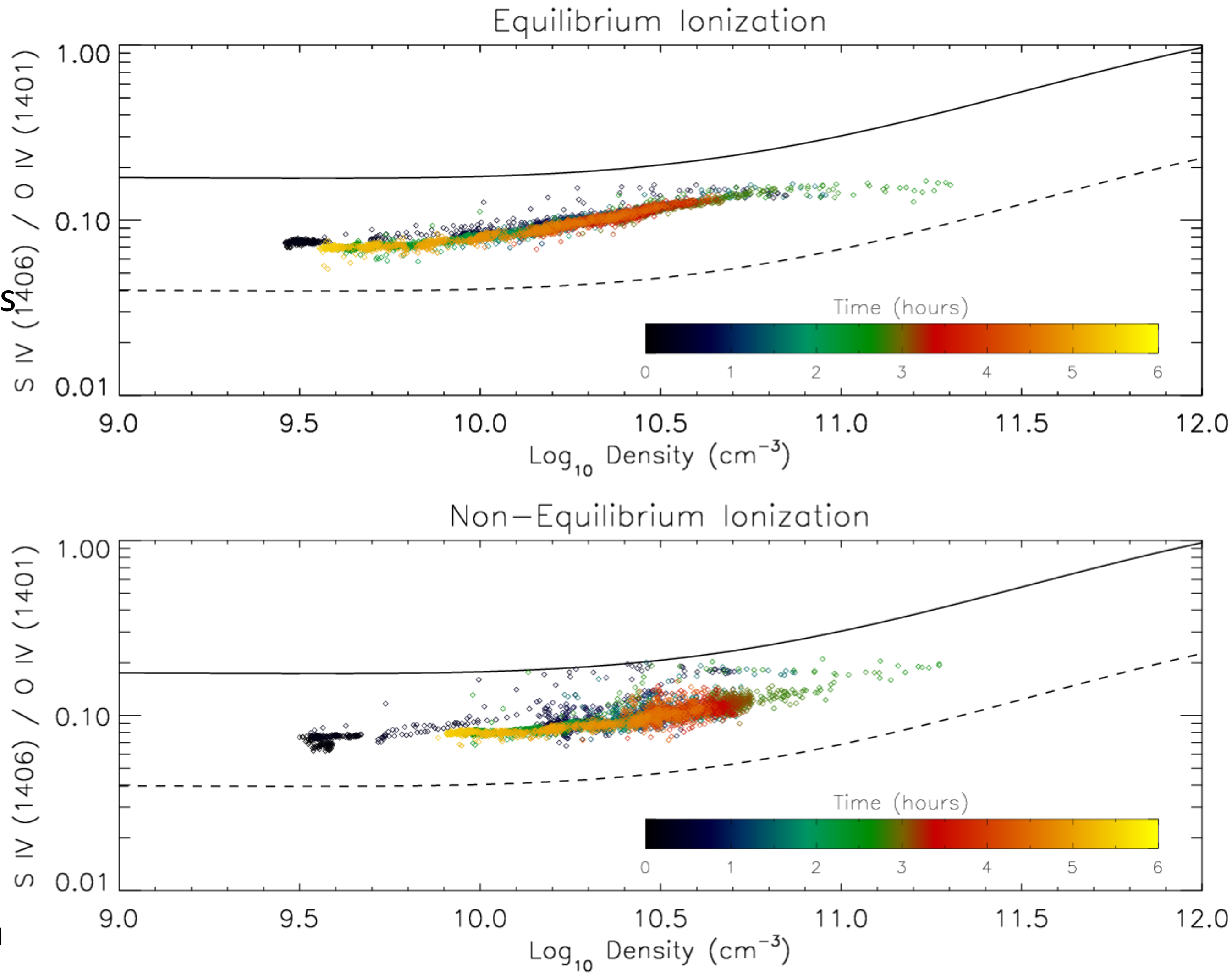

[8] Dere, K. P., et al. 1997, A&AS, 125, 149 ; [9] Dere K. P., et al. 2019, A&AS, 241, 2

ADAS Rates, Weak Heating, Density Dependent

The intensity ratios of the S IV (1406.060 Å) and O IV (1401.163 Å) lines plotted as a function of the electron density calculated using the O IV (1404.806 / 1399.776 Å) line ratio.

Solid: Chianti-predicted ratio at the S IV equilibrium formation temperature ($\log_{10}T = 5.0$ K).

Dashed: Chianti-predicted ratio at the O IV equilibrium formation temperature ($\log_{10}T = 5.15$ K).

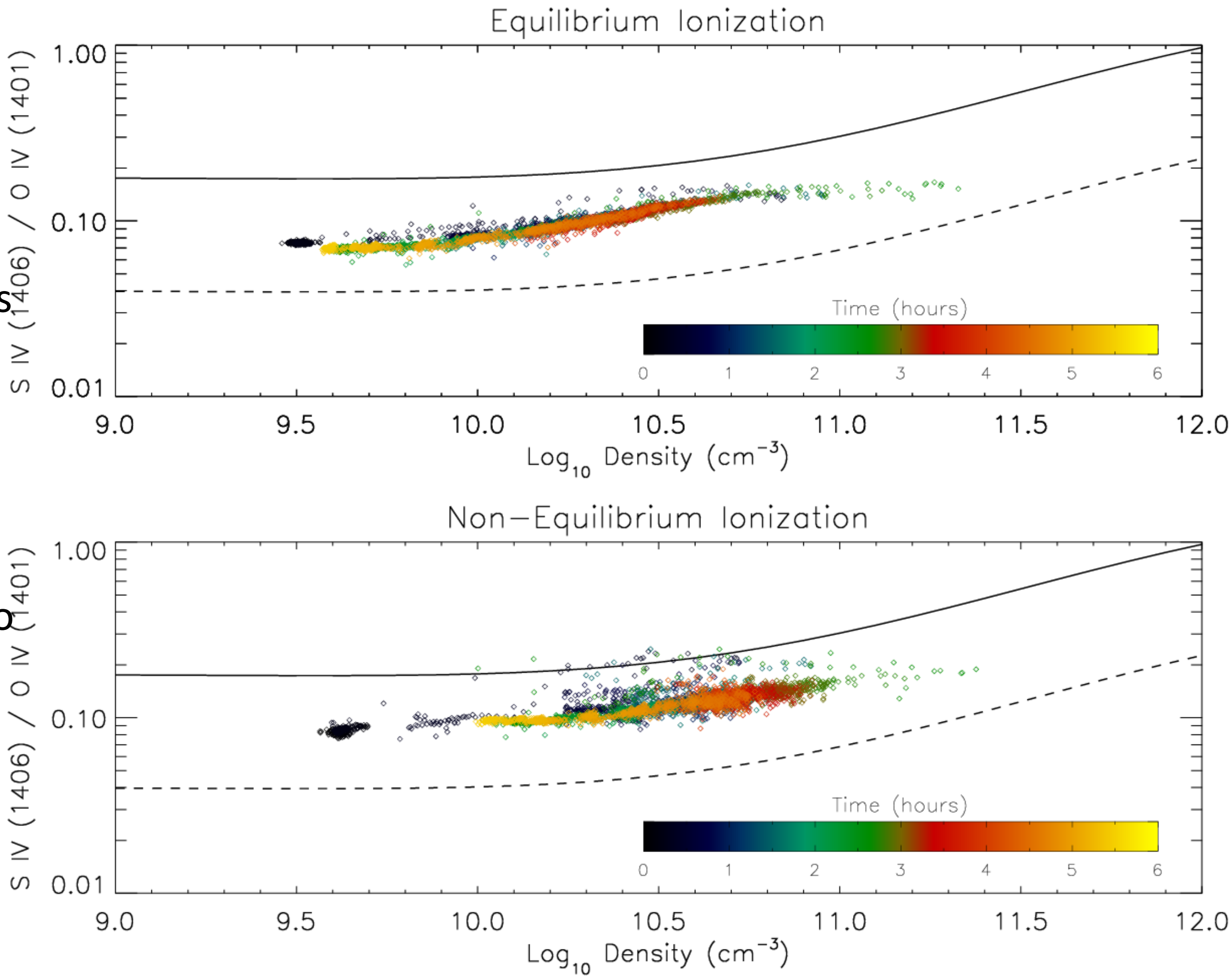

ADAS Rates, Weak Heating

The maximum intensity of the S IV (1406.060 Å) and O IV (1401.163 Å) lines as a function of electron density.

Red – low-density limit
Blue – density dependent
Purple – regions of overlap

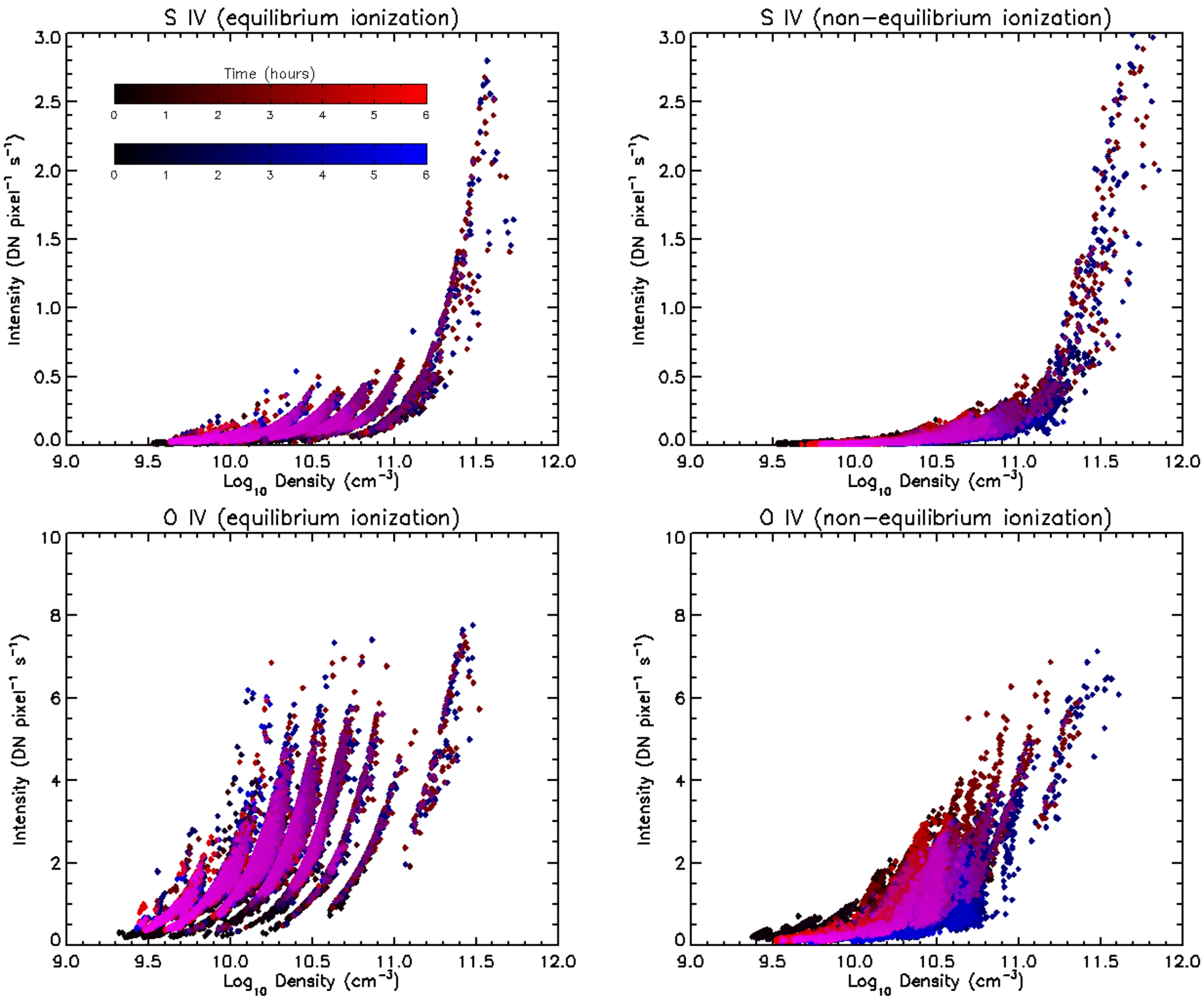

ADAS Rates, Weak Heating

The maximum intensity of the S IV (1406.060 Å) and O IV (1401.163 Å) lines as a function of electron temperature.

Red – low-density limit
Blue – density dependent
Purple – regions of overlap

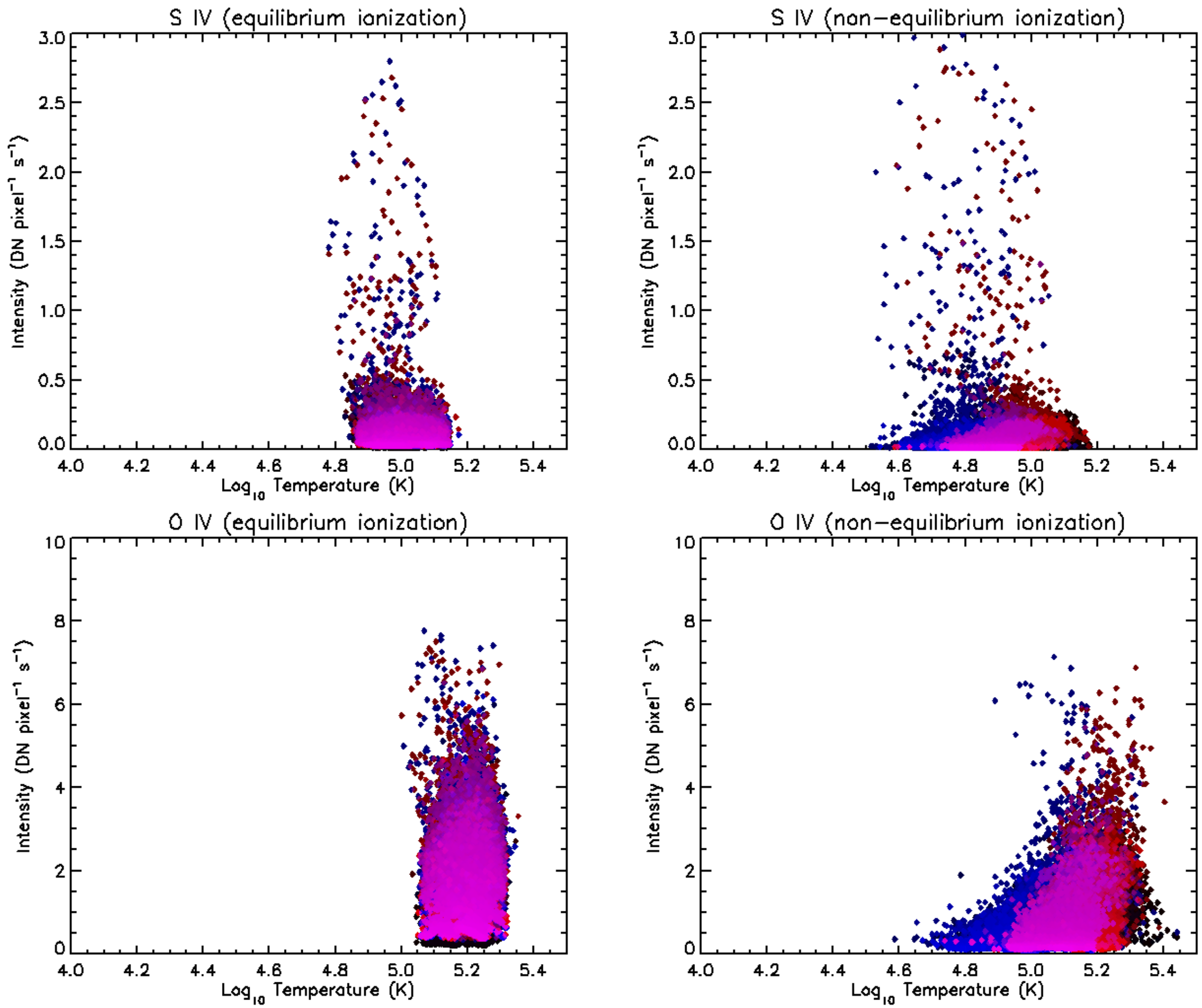

2. Heating in the Transition Region

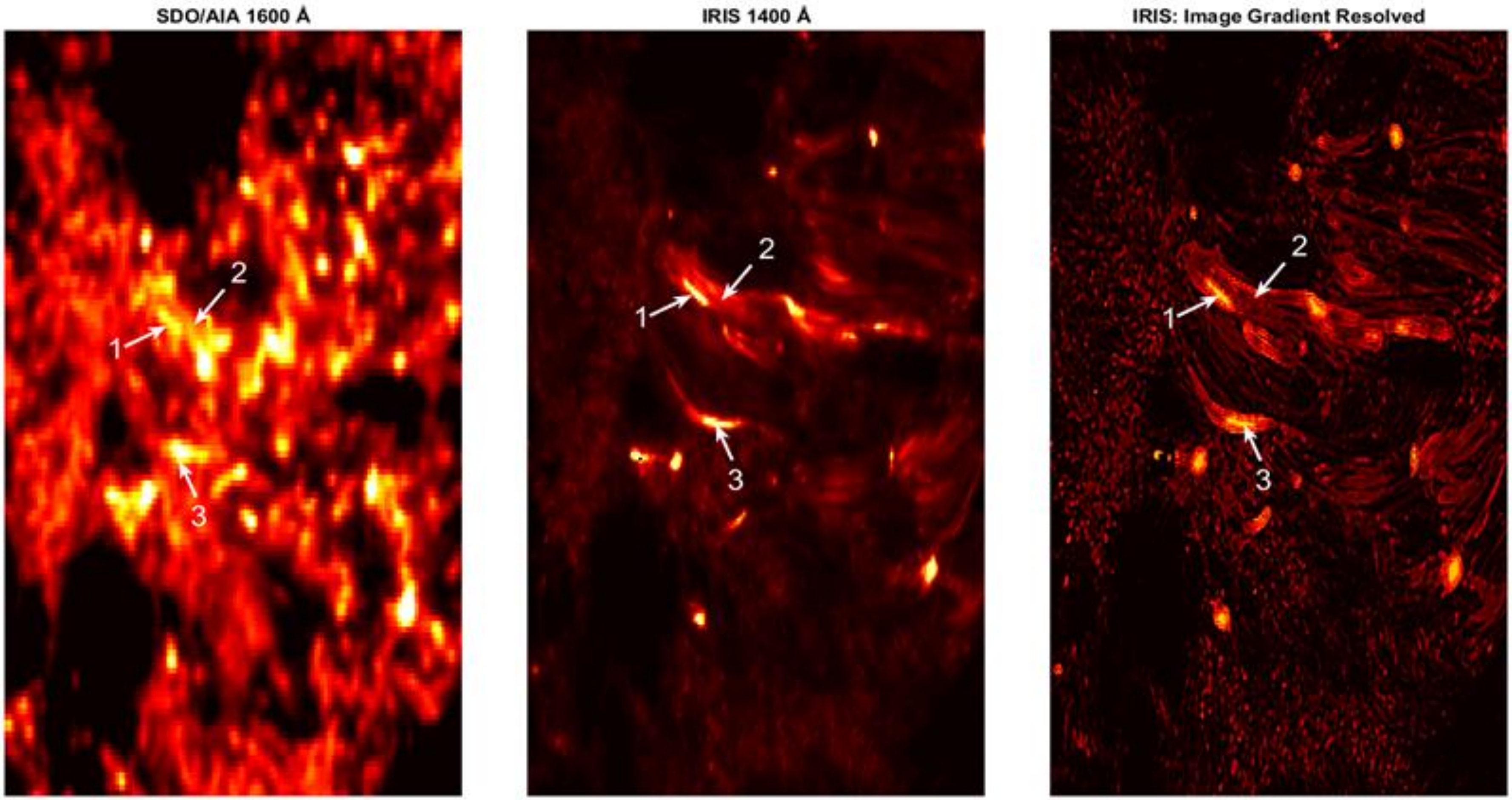

2a. IRIS Observations

Two-component fit to Si IV 1403 Å (max. |v| = 100 km/s)

Position 1

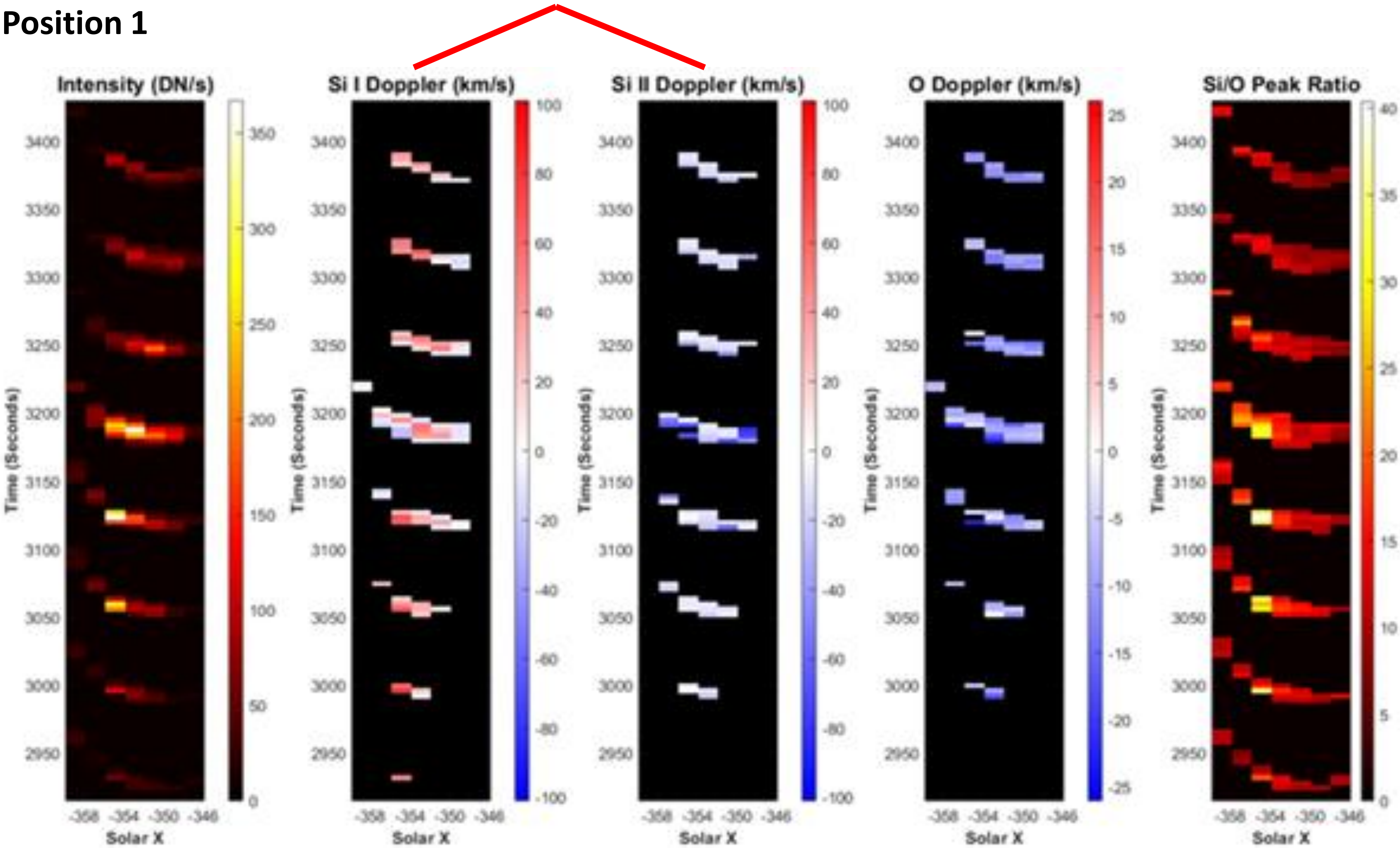

Position 2

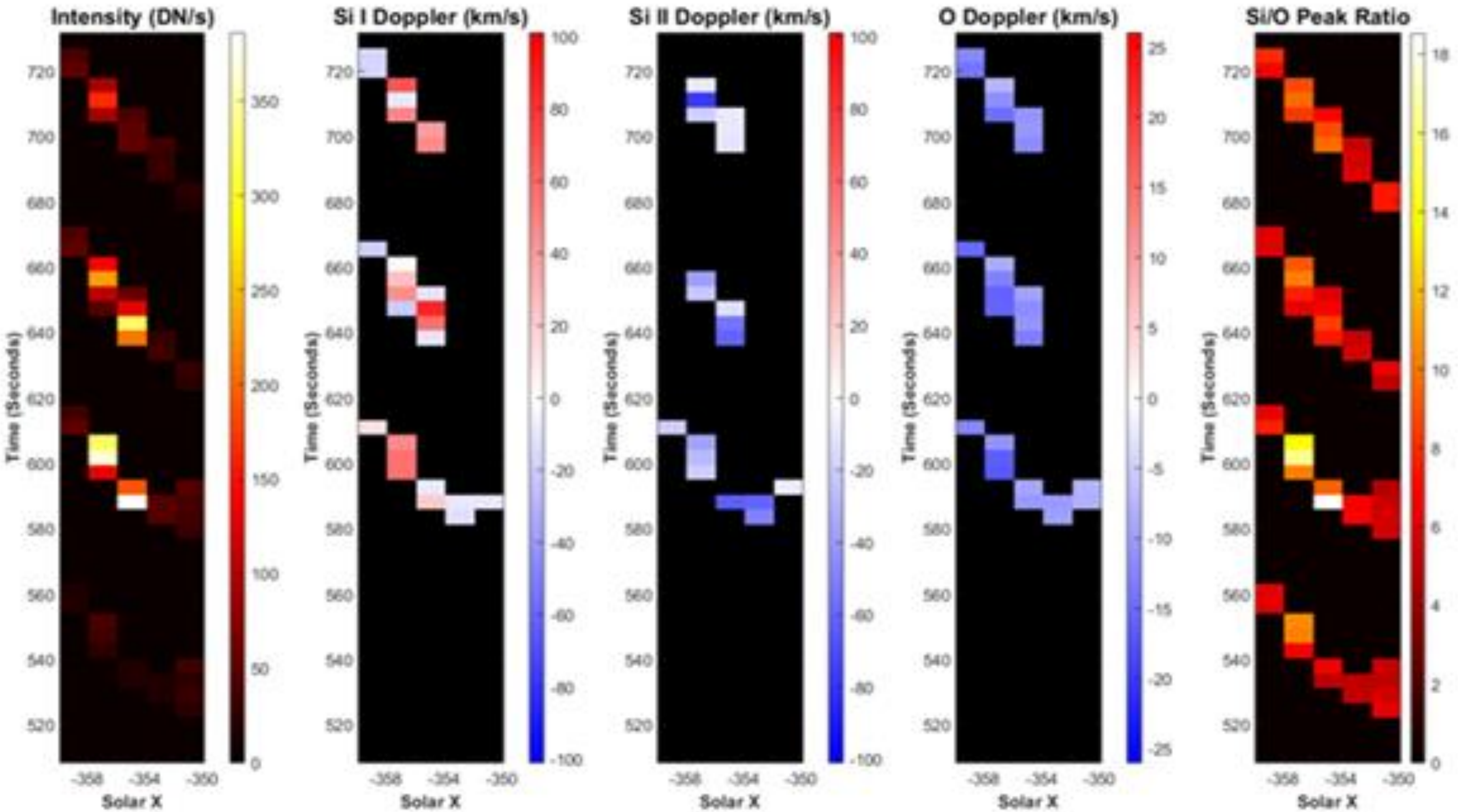
Intensity (DN/s)
Si I Doppler (km/s)
Si II Doppler (km/s)
O Doppler (km/s)
Si/O Peak Ratio
Time (Seconds)
Solar X

2b. Numerical Investigation

1st observational constraint: high density (10^{10} - 10^{11} cm^{-3}) at apex

- foot-point heating by a train of impulsive events to create a condensation

2nd constraint: fast bidirectional flow in bright apex pixels

- heating by a train of impulsive events at the condensation site

3rd constraint: high Si IV/O IV

- consider atomic processes including non-equilibrium ionization and density-dependent rates

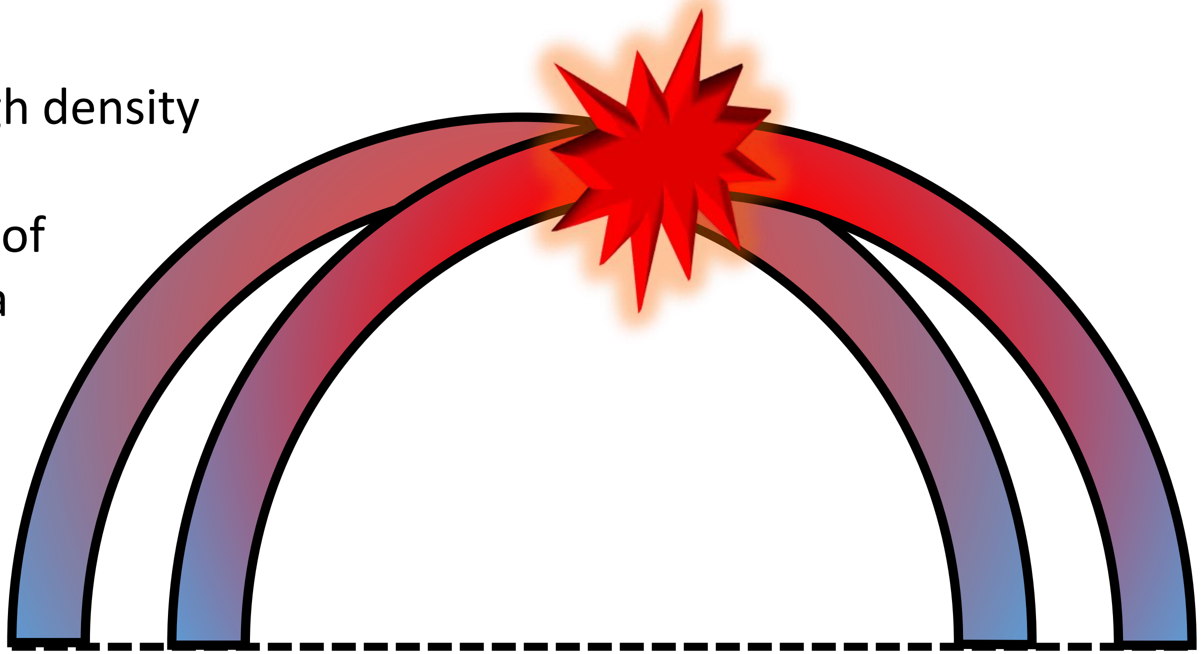

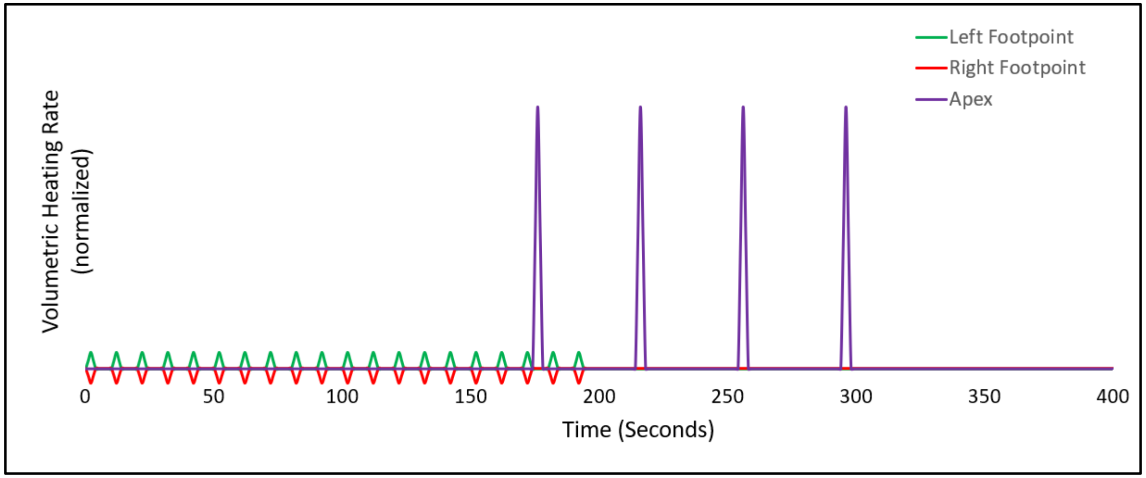

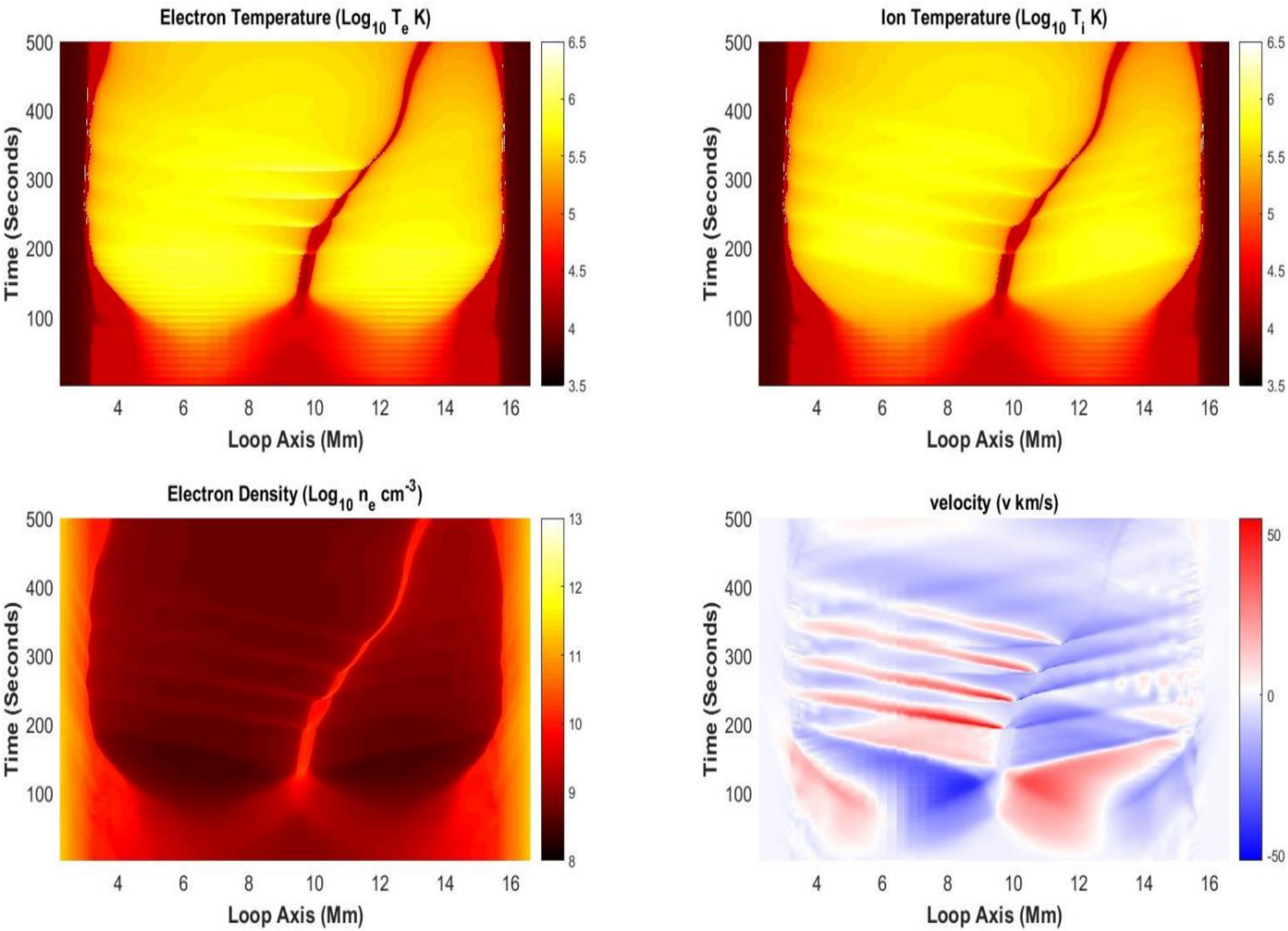
Electron Temperature (Log_{10} T_e K)
Ion Temperature (Log_{10} T_i K)
Electron Density (Log_{10} n_e cm^{-3})
velocity (v km/s)
Time (Seconds)
Loop Axis (Mm)
500
400
300
200
100
4
6
8
10
12
14
16
6.5
6
5.5
5
4.5
4
3.5
13
12
11
10
9
8
50
0
-50

Equilibrium ionization with rates in the low density limit

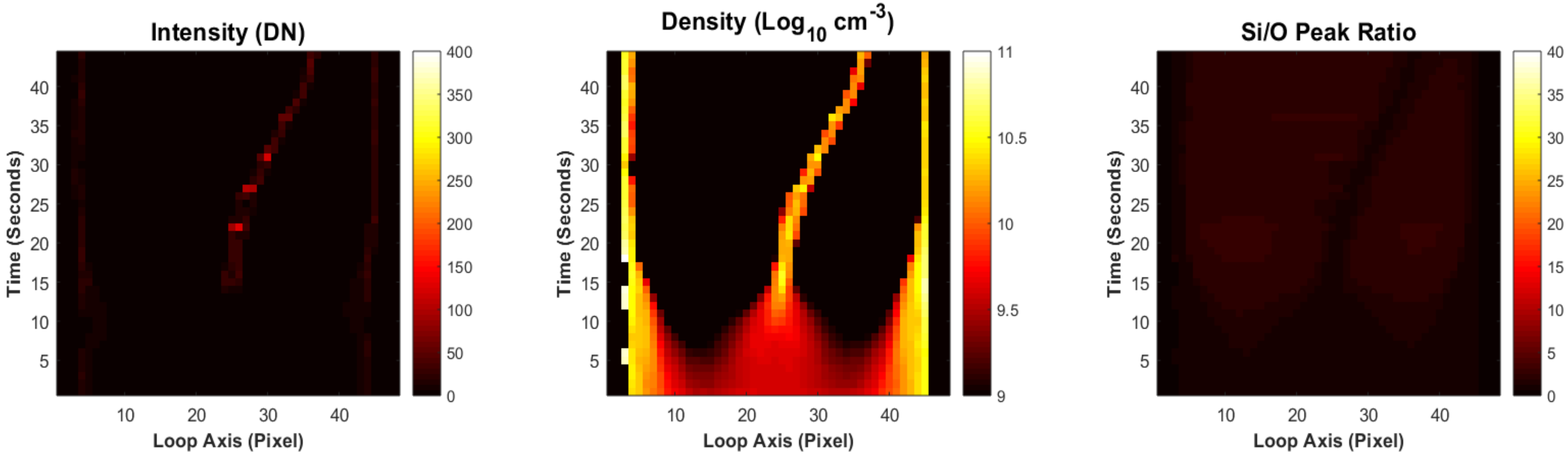

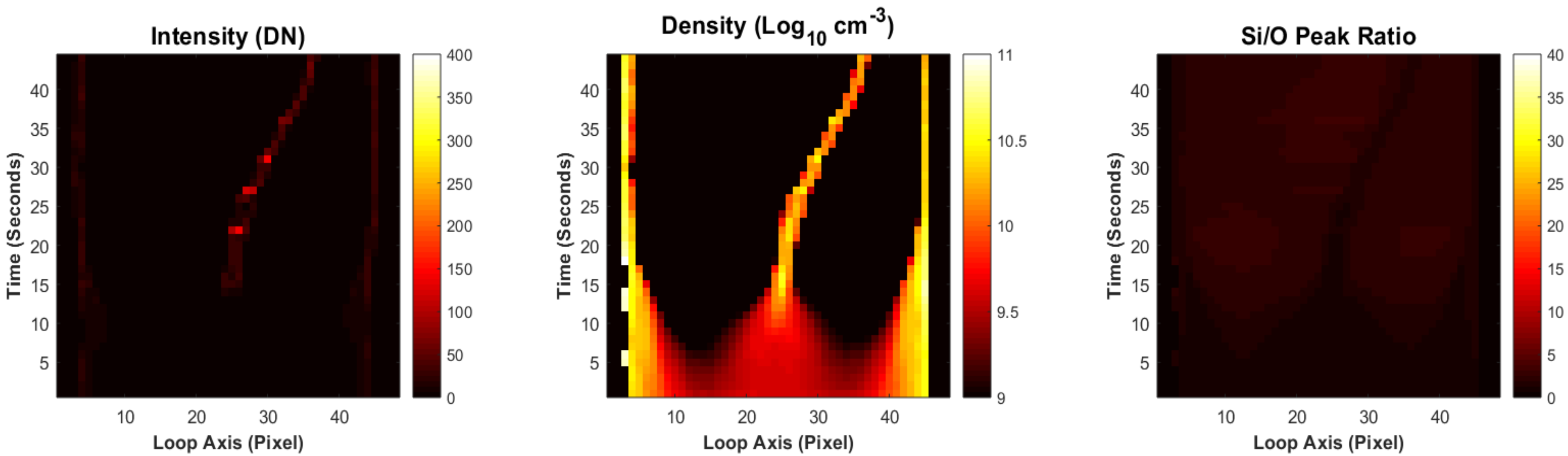

Non-equilibrium ionization with rates in the low density limit

Equilibrium ionization with density-dependent rates

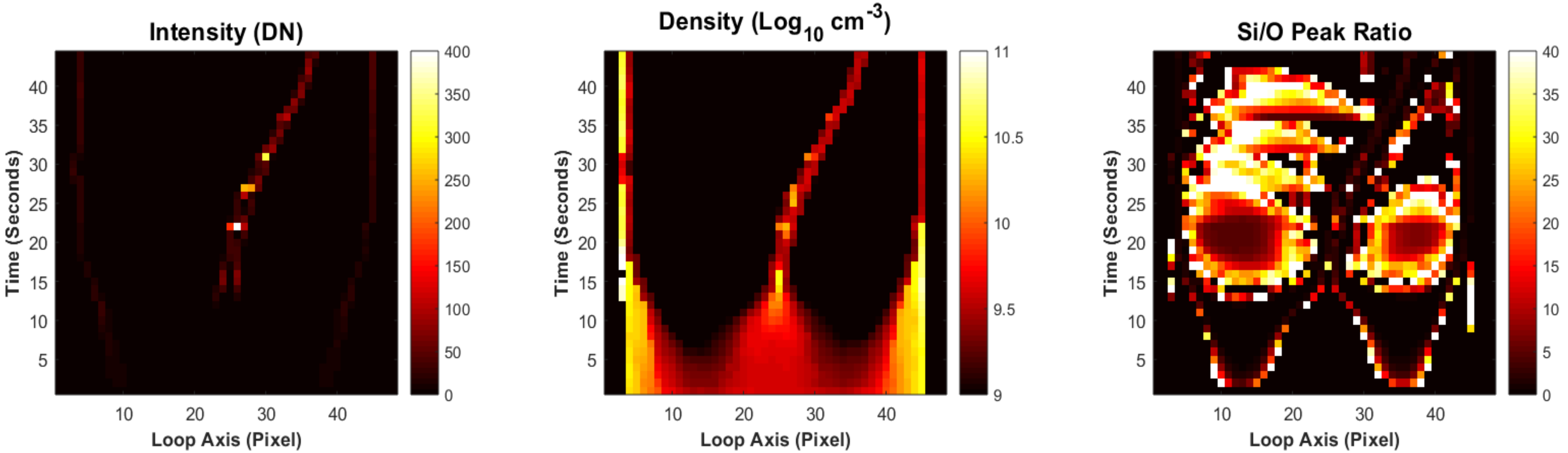

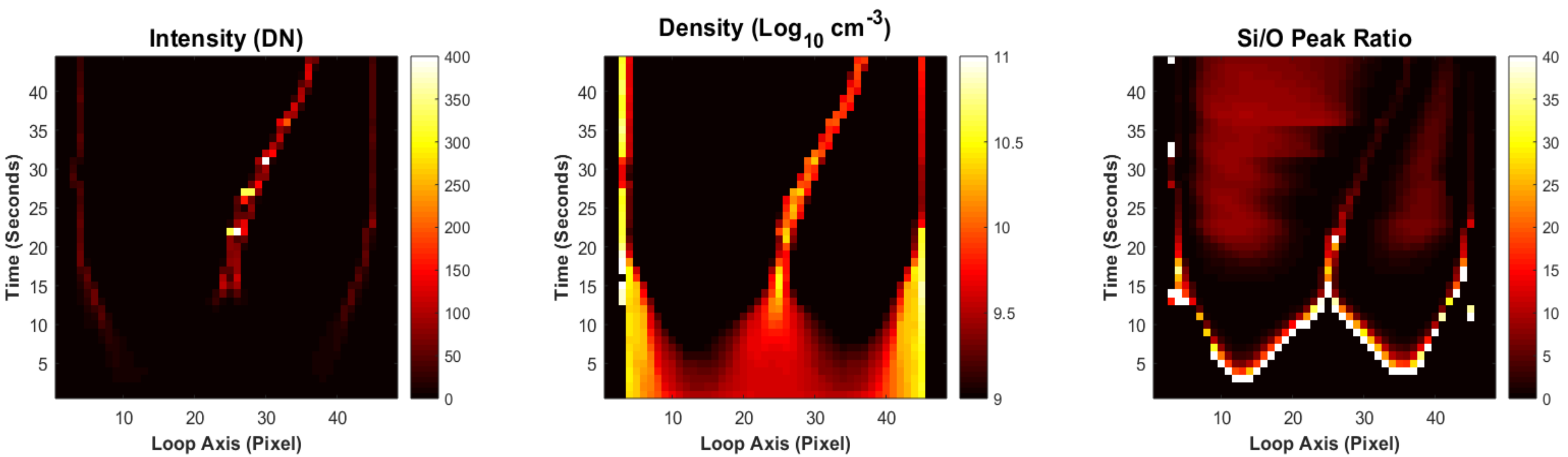

Non-equilibrium ionization with density-dependent rates

	Density Log n_e (cm^{-3})	**Intensity** $(\mathrm{DN/s})$	**Si/O Peak Ratio**
Measured by IRIS	10.5 – 13	180 – 700	16 – 70
Equilibrium Ionization Low Density (LD) Rate Limit	10.5 – 11	68	2
Non-equilibrium Ionization Low-density (LD) Rate Limit	10.5 – 11	80	3
Equilibrium Ionization Density-dependent (DD) Rates	9.8 – 10.5	200	14
Non-equilibrium Ionization Density-dependent (DD) Rates	10 – 10.7	400	40

3. Summary of Findings

- Line intensities and plasma properties can be grossly mis-calculated when transition region atomic processes are ignored
- Transition region lines can form over a much broader range of densities and temperatures than predicted in equilibrium
- The effects of density-dependent processes are greatly enhanced when coupled to non-equilibrium ionization (NEQI)
- The distribution of data points produced by the S IV / O IV ratio vs. density is sensitive to the strength of NEQI and could provide important diagnostics
  - Density-dependent distribution tends to ratio curve at S IV equilibrium temperature
- Model predictions are only consistent with the large measured Si IV / O IV ratio for NEQI and density-dependent rates
- Next steps: more comparisons between models and IRIS observations, under these constraints, to find heating properties